# Stretch Harmonizes Sarcomere Strain Across the Cardiomyocyte

Jia Li, Joakim Sundnes, Yufeng Hou, Martin Laasmaa, Marianne Ruud, Andreas Unger, Terje Kolstad, Michael Frisk, Per Norseng, Limin Yang, et al.

# Stretch Harmonizes Sarcomere Strain Across the Cardiomyocyte

Jia Li [1 2], Joakim Sundnes [# 3], Yufeng Hou [# 1 2], Martin Laasmaa [1 2], Marianne Ruud [1 2], Andreas Unger [4], Terje R Kolstad [1 2], Michael Frisk [1 2], Per Andreas Norseng [1], Limin Yang [5], Ingunn E Setterberg [1 2], Estela S Alves [6], Michaeljohn Kalakoutis [6], Ole M Sejersted [1 2], Johanna T Lanner [6], Wolfgang A Linke [4], Ida G Lunde [1 2], Pieter P de Tombe [7 8], William E Louch [1 2]

[1] Institute for Experimental Medical Research, Oslo University Hospital and University of Oslo, Norway (J.L., Y.H., M.L., M.R., T.R.K., M.F., P.A.N., I.E.S., O.M.S., I.G.L., W.E.L.).

[2] KG Jebsen Center for Cardiac Research, University of Oslo, Norway (J.L., Y.H., M.L., M.R., T.R.K., M.F., I.E.S., O.M.S., I.G.L., W.E.L.).

[3] Simula Research Laboratory, Lysaker, Norway (J.S.).

[4] Institute of Physiology II, University of Münster, Germany (A.U., W.A.L.).

[5] DNV, Høvik, Norway (L.Y.).

[6] Department of Physiology and Pharmacology, Karolinska Institutet, Stockholm, Sweden (E.S.A., M.K., J.T.L.).

[7] Department of Physiology and Biophysics, University of Illinois at Chicago (P.P.d.T.).

[8] Phymedexp, Université de Montpellier, INSERM, CNRS, France (P.P.d.T.).

[#] **Contributed equally.**
* J. Sundnes and Y. Hou **contributed equally**

**Keywords:**

connectin; myocytes, cardiac; sarcomeres.

**Correspondence to:**

Jia Li, PhD, Institute for Experimental Medical Research, Oslo University Hospital, Ullevål, Kirkeveien 166, NO-0407 Oslo, Norway, Email jia.li@medisin.uio.no or William E. Louch, PhD, Institute for Experimental Medical Research, Oslo University Hospital, Ullevål, Kirkeveien 166, NO-0407 Oslo, Norway, Email w.e.louch@medisin.uio.no.

**Nonstandard Abbreviations and Acronyms**

| | |
|---|---|
| **LDA** | length-dependent activation |
| **MyBP-C** | myosin binding protein C |
| **SL** | sarcomere length |
| **WT** | wild type |

# Abstract

**Background:**

Increasing cardiomyocyte contraction during myocardial stretch serves as the basis for the Frank-Starling mechanism in the heart. However, it remains unclear how this phenomenon occurs regionally within cardiomyocytes, at the level of individual sarcomeres. We investigated sarcomere contractile synchrony and how intersarcomere dynamics contribute to increasing contractility during cell lengthening.

**Methods:**

Sarcomere strain and $Ca^{2+}$ were simultaneously recorded in isolated left ventricular cardiomyocytes during 1 Hz field stimulation at 37 °C, at resting length and following stepwise stretch.

**Results:**

We observed that in un-stretched rat cardiomyocytes, differential sarcomere deformation occurred during each beat. Specifically, while most sarcomeres shortened during the stimulus, ≈10% to 20% of sarcomeres were stretched or remained stationary. This nonuniform strain was not traced to regional $Ca^{2+}$ disparities but rather shorter resting lengths and lower force production in systolically stretched sarcomeres. Lengthening of the cell recruited additional shortening sarcomeres, which increased contractile efficiency as less negative, wasted work was performed by stretched sarcomeres. Given the known role of titin in setting sarcomere dimensions, we next hypothesized that modulating titin expression would alter intersarcomere dynamics. Indeed, in cardiomyocytes from mice with titin haploinsufficiency, we observed greater variability in resting sarcomere length, lower recruitment of shortening sarcomeres, and impaired work performance during cell lengthening.

**Conclusions:**

Graded sarcomere recruitment directs cardiomyocyte work performance, and harmonization of sarcomere strain increases contractility during cell stretch. By setting sarcomere dimensions, titin controls sarcomere recruitment, and its lowered expression in haploinsufficiency mutations impairs cardiomyocyte contractility.

## Novelty and Significance

### What Is Known?

- During increased ventricular filling, greater cardiac output defined by the Frank-Starling law is provided by length-dependent activation (LDA) of sarcomeres, the contractile units within cardiomyocytes.
- A variety of mechanisms have been proposed to underlie LDA, including central roles of the giant elastic protein titin in controlling sarcomere geometry and force development.
- However, it remains unclear how intersarcomere dynamics regulate this phenomenon.

### What New Information Does This Article Contribute?

- We observed that in cardiomyocytes at resting length, ≈10% to 12% of sarcomeres exhibit stretch instead of shortening, due to their shorter resting lengths and lower force production.
- LDA is linked to recruitment of sarcomeres, which increases contractile efficiency and work performance.
- Lowered titin expression resulting from haploinsufficiency mutation results in greater variability in resting sarcomere length and less recruitment of shortening sarcomeres during LDA.

Increased filling of the ventricles with blood, and the resulting stretch of cardiomyocytes, increases cardiac output according to the Frank-Starling Law. But what are the sub-cellular mechanisms for this phenomenon? Much previous work has revealed important roles of changes in $Ca^{2+}$ sensitivity of the myofilaments and increasing force development. The present results show a novel aspect of LDA; namely that cell lengthening recruits more sarcomeres to shorten. Why does this occur? We observed that variability in sarcomere length is key. In cells at resting length, sarcomeres which are shorter than average produce lower force, and are more likely to be stretched by their longer, more forceful neighbors. However, when the cell is lengthened, increasing force production in these sarcomeres enables more of them to contract, and overall cellular contractility is increased. Can alterations in this mechanism be pathological? Yes. We observed that lowered titin expression due to haploinsufficiency mutations results in greater variability in sarcomere length and an increased proportion of stretched sarcomeres. These results point to an important role of titin in regulating sarcomere recruitment during LDA, and a new understanding of impaired cardiac performance in individuals with titin truncation mutations.

Cardiac myocytes are composed of repeating contractile units called sarcomeres. Within each sarcomere, actin and myosin are organized into a hexagonal lattice pattern, with 6 actin thin filaments positioned around each myosin thick filament.[1,2] Sarcomeric contraction is triggered by a rise in cytosolic $Ca^{2+}$ levels, as influx via L-type $Ca^{2+}$ channels triggers additional $Ca^{2+}$ release from ryanodine receptors in the sarcoplasmic reticulum.[3] Binding of released $Ca^{2+}$ to troponin C on the actin filament allows crossbridge formation with myosin heads, initiating force development and contraction.[4–6] The summation of force generated by parallel sarcomeres determines the force production of the whole cell.

In the healthy heart, sarcomere contraction is tightly regulated to meet cardiac demand. For example, during increased ventricular filling, greater cardiac output defined by the Frank-Starling law is provided by length-dependent activation (LDA) of sarcomeres.[7] While the precise mechanisms underlying LDA remain debated, experiments based on skinned cardiac trabeculae have shown that increasing sarcomere length (SL) augments both myofilament $Ca^{2+}$ sensitivity and maximal developed force.[7–12] Increased myofilament $Ca^{2+}$ responsiveness has, in turn, been linked to a reduction of interfilament lattice spacing during stretch and an increased likelihood of crossbridge formation.[13] However, LDA may involve additional mechanisms,[14] since stretch causes critical structural changes in both the thin and thick filaments.[15,16] Specifically, stretch induced conformational changes in troponin C have been linked to increased myofilament $Ca^{2+}$ sensitivity,[11] while force-dependent recruitment of myosin heads from the off to on state[17–19] is reported to increase maximal developed force.[11]

The proposed LDA mechanisms described above are suggested to critically involve the elastic sarcomeric protein titin. Due to its oblique positioning between actin attachment sites in the Z disc and the thick filaments in the A band, stretch causes titin to pull the thick and thin filaments together, reducing lattice spacing. However, titin also binds to MyBP-C (myosin-binding protein C).[20] Resulting strain transduction during SL is proposed to facilitate transition of myosin heads to the on state, while also enabling MyBP-C binding to the thin filaments, altered troponin configuration, and thin filament activation.[21] Although the details of these mechanisms require further investigation, there is general agreement that long, compliant titin variants weaken LDA by reducing longitudinal strain transduction.[15,22–24] Similarly, acute cleavage of 50% of the titin springs attenuates LDA, at least in skeletal muscle.[25] While the described studies have provided important insight into how LDA may occur at the level of the single sarcomere, it has remained unclear whether and how these effects are synchronized between adjoining sarcomeres to increase whole-cell force development and contractility. In the present study, we demonstrate that unstretched cardiomyocytes in fact exhibit nonhomogeneous sarcomeric function, as shorter sarcomeres are stretched during systole by their longer, shortening neighbors. We show that LDA includes harmonization of sarcomere strain across the cell, as progressively more sarcomeres are recruited to shorten, increasing work performance. Graded sarcomere recruitment is dependent on variable SL at baseline, which is regulated by titin. We observed that abnormally reduced titin expression, as occurs following haploinsufficiency mutation,[26–28] increases variability in SL, diminishes collaboration between sarcomeres, and impairs cardiomyocyte work performance.

# Methods

## Data Availability

The data that support the findings of this study are available from the corresponding authors upon reasonable request. Additional methods are described in the Supplemental Material.

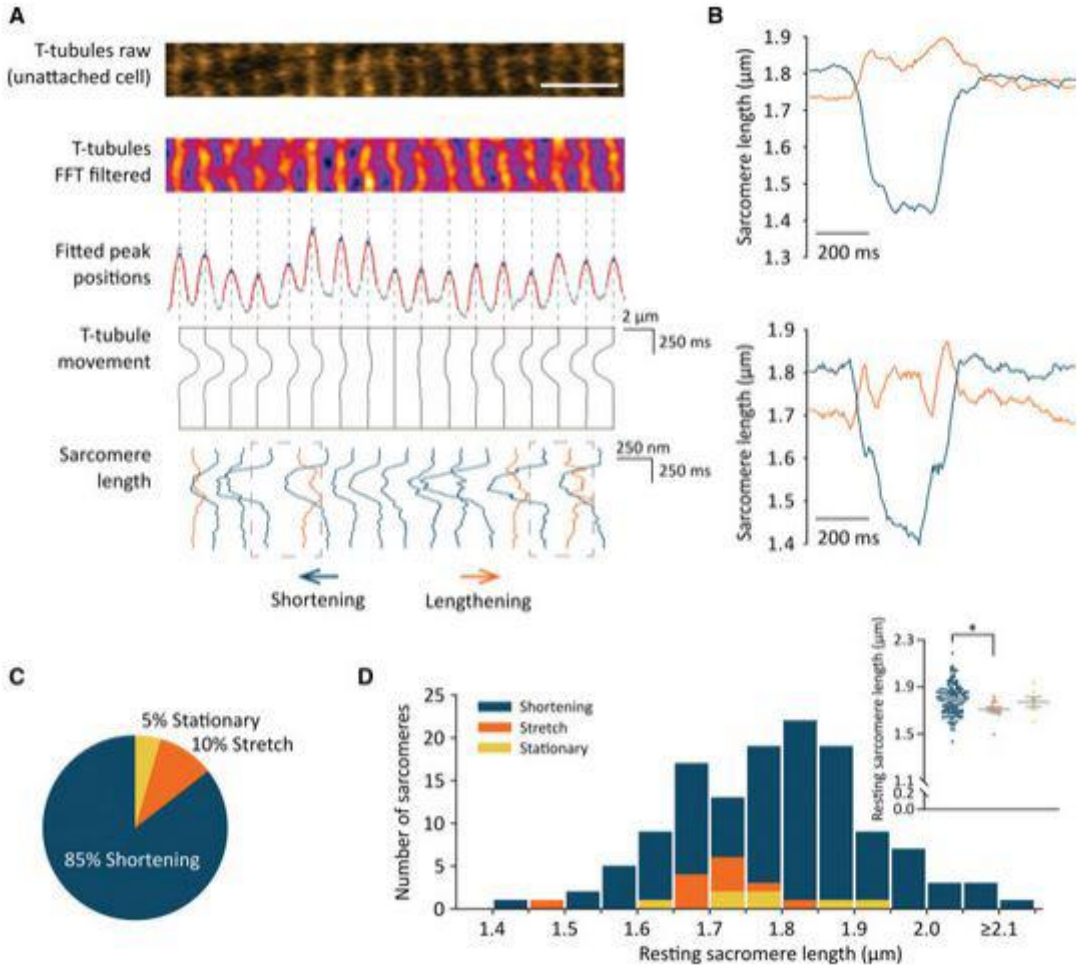


**Figure 1**. **Healthy cardiomyocytes exhibit nonuniform sarcomere strain. A**,

Sarcomeres in isolated cardiomyocytes were tracked by CellMask labeling of t tubules. High-speed confocal imaging of 2-dimensional regions was performed during 1 Hz field stimulation at 37 °C (scale bar, 5 µm). Parabolic fitting was used to identify peak transverse signals, with each peak defining a Z-line position (original data, gray; fitted curve, red; fitted peak, dark blue; see also Figure S1). By subtracting neighboring Z-line positions, sarcomere length (SL) change traces were plotted. During cell contraction, most sarcomeres shortened normally (dark blue traces in **bottom**), but some sarcomeres were lengthened (orange traces). **B**, Sarcomere deformations from neighboring sarcomeres are plotted in the same graphs, from 2 regions indicated in **A** (dashed gray frames). **C**, Proportions of sarcomeres exhibiting shortening, stretch, or no change in length. **D**, Resting SLs were observed to be nonhomogeneous, and stretched sarcomeres were significantly shorter than those that shortened. Data are presented as mean ± SEM together with raw data. $n_{sarcomeres}$: shortening, 130; stretch, 15; stationary, 7 from 13 cells, 5 hearts. Statistical analysis was performed by linear mixed model. $P<0.05$ was considered significant (*$P<0.05$). Detailed statistical results are shown in Table S1.

# Results

**Cardiomyocytes Exhibit Nonuniform Sarcomere Strain**

We examined the dynamics of individual sarcomeres in isolated rat cardiomyocytes during 1 Hz pacing. In initial experiments, Z-line positions were estimated using t-tubule staining (CellMask) and rapid 2-dimensional confocal scanning of cells plated on coverslips (Figure 1A). Sarcomere strain was calculated using the relative change in position of the neighboring t tubules (Methods; Figure S1). Surprisingly, these analyses revealed nonuniform sarcomere deformation across the contracting cell, as indicated by representative traces in Figure 1A and enlargements presented in Figure 1B. Specifically, while most sarcomeres shortened during the stimulus (85%), a significant portion was observed to be stretched (10%) or remain stationary (5%; Figure 1C). The presented traces also highlight that complex strain patterns can occur at the level of single sarcomeres, including phases of shortening despite net single sarcomere stretch. Notably, the resting SL of sarcomeres that were stretched during systole was observed to be significantly shorter than those that shortened (Figure 1D).

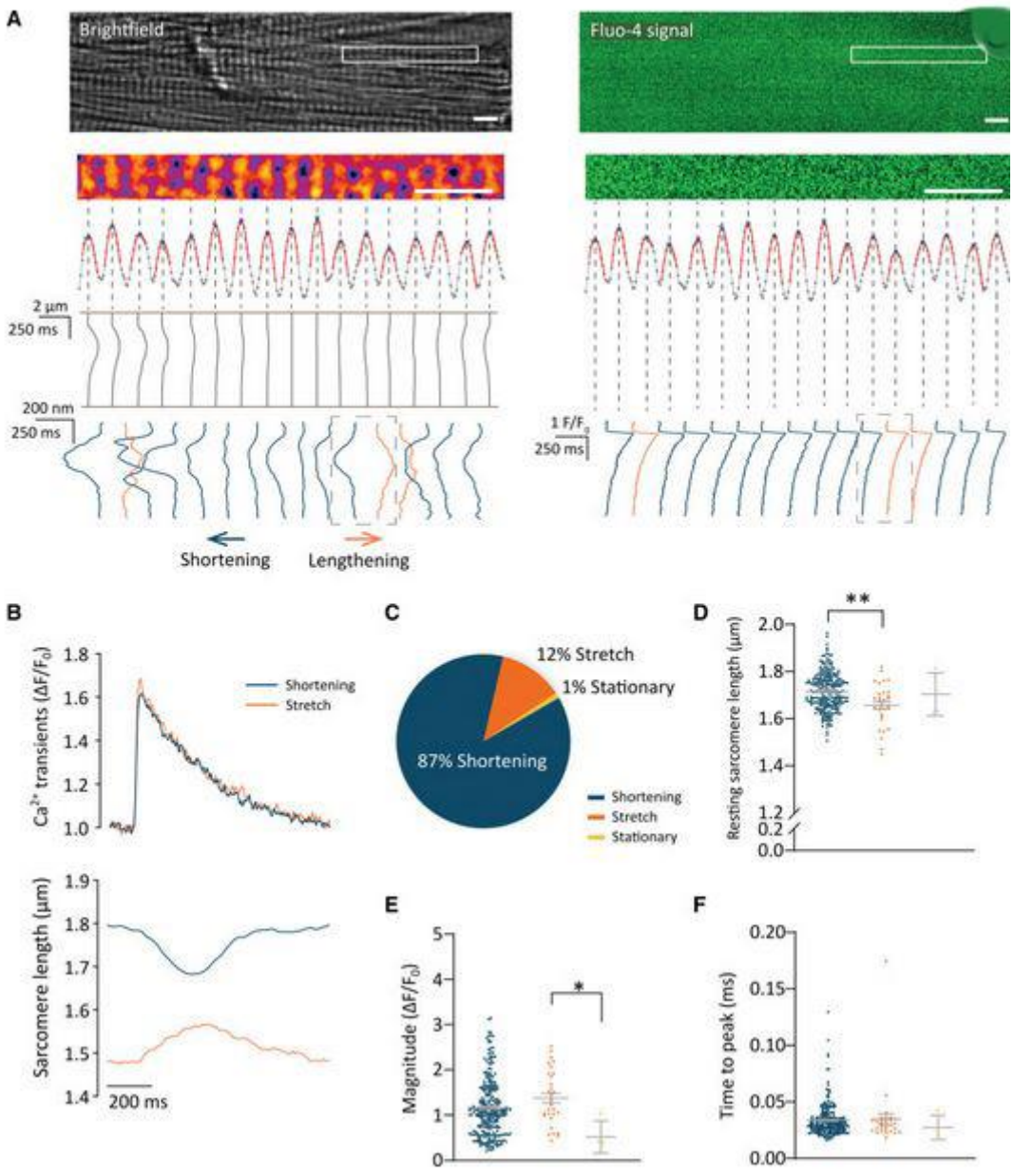

**Figure 2**. **Differential sarcomere deformation occurs despite uniform Ca2+ transients. A**, Epifluorescent microscopy was used to simultaneously monitor cytosolic Ca2+ and sarcomere striations, using fluo-4 fluorescence and bright-field signals, respectively (see also Figure S2). Bright-field images (**left**) were filtered with a fast Fourier transform and inverted to assign Z-line signals the highest values (orange). Parabolic fitting was performed to identify peak transverse signals, defining Z-line positions (original data, gray; fitted curve, red; fitted peak, dark blue). By averaging Z-line movement from 5 consecutive contractions, sarcomere deformation traces were plotted. Z-line positions were also used to define local Ca2+ transients for each sarcomere (**right**; fluorescence at peak of the Ca2+ transient is illustrated at the **top**). Despite uniform Ca2+ transients observed at individual sarcomeres, differential sarcomere strain was observed (**bottom**). Scale bars, 5 μm. **B**, Local Ca2+ transients and deformations from the neighboring sarcomeres indicated in **A** (dashed gray frames) are plotted in the same graph. **C**, Proportions of sarcomeres exhibiting shortening, stretch, or no change in length, as determined by bright-field measurements of Z-line positions. **D**, The resting sarcomere length of stretched sarcomeres was significantly shorter than those that shortened. Ca2+ transient magnitude (**E**) and time to peak (**F**) for individual sarcomeres. Data are presented as mean ± SEM together with raw data. $n_{sarcomeres}$: shortening, 233; stretch, 31; stationary, 4, from 17 cells, 6 hearts. Statistical analysis was performed by linear mixed model (**D**) or Kruskal-Wallis test with Dunn corrections (**E** and **F**). $P<0.05$ was considered significant (*$P<0.01$, **$P<0.01$). Detailed statistical results are shown in Tables S2 through S4.

As t-tubule morphology deforms during cardiomyocyte contraction,[29] we next sought to support our above observations using direct visualization of Z lines by transmitted light (method described in Figure S2). Representative recordings (Figure 2A, enlargements in Figure 2B) and overall data (Figure 2C) show that, as in t-tubule tracking experiments, sarcomeres can exhibit shortening, stretch, or maintained length during the electrical stimulus (87%, 12%, and 1% of sarcomeres, respectively). Z-line tracking also confirmed that, before the stimulus, stretched sarcomeres exhibit significantly shorter resting lengths than those that shortened (Figure 2D). Importantly, the observed nonuniform pattern of sarcomere strain was highly consistent over time, as 98.9% of sarcomeres were found to maintain either positive or negative strain during consecutive beats (Figure S2E and S2F). These analyses further showed that this method of Z-line tracking over consecutive beats allows small changes in SL to be detected (Figure S2G).

An advantage of the transmitted light approach to Z-line tracking is that it enables simultaneous assessment of local Ca2+ transients (fluo-4), with splitting of the 2 signals onto a high-speed camera (Methods). Paired traces presented in Figure 2B show that local Ca2+ transients measured within sarcomeres that stretched during systole were nearly identical to those recorded in their shortening neighbors. Mean data supported that the magnitude and kinetics of Ca2+ release were similar in these 2 groups of sarcomeres (Figure 2E and 2F). These findings suggest that nonuniform sarcomere strain does not result from local differences in Ca2+ transients but rather may involve differences in resting length. Specifically, long sarcomeres that produce significant force may shorten at the expense of shorter sarcomeres, which produce little force and are stretched.

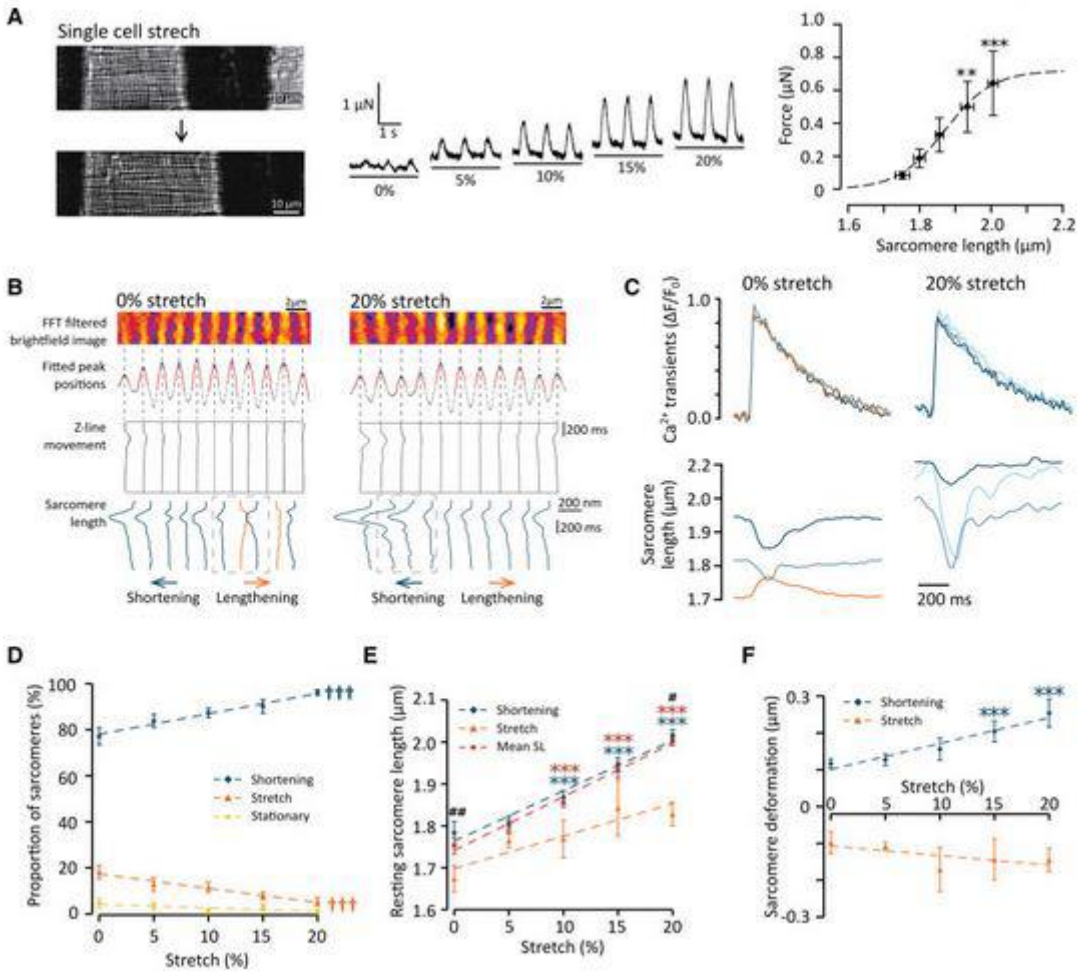


**Figure 3**. **Length-dependent activation in single cardiomyocytes is associated with harmonization of sarcomere strain. A**, Cardiomyocytes were attached to glass fibers and stretched in intervals corresponding to a 5% command increase in length. Developed force recordings are presented for the illustrated cardiomyocyte, with data (mean ± SEM) presented at **right** (sigmoidal curve fitting; see Figure S4 for raw recording). **B**, Sarcomere deformations in a representative cardiomyocyte at 0% and 20% stretch. **C**, Local Ca2+ transients and sarcomere deformations from the neighboring sarcomeres indicated in **B. D**, Progressive stretch increased the proportion of sarcomeres exhibiting shortening. **E**, During cell stretch, resting sarcomere length remained longer in shortening than stretched sarcomeres. **F**, Increasing magnitude sarcomere shortening during cell lengthening. Data in **D** through **F** are presented as mean ± SEM with regression line. The same sarcomeres were examined in all panels. $n_{sarcomeres}$: 0% stretch, 86; 5% stretch, 100; 10% stretch, 100; 15% stretch, 109; 20% stretch, 121, from = 6 cells, 6 hearts. Statistical methods: (**A**) 1-way repeated measures ANOVA to test the hypothesis that cell stretch increased force development in comparison with the un-stretched (0%) state; (**D**) linear mixed models; (**E**) and (**F**) Kruskal-Wallis method for comparisons within each group and Mann-Whitney method for comparisons between groups. $P<0.05$ was considered significant. $^{**}P<0.01$, $^{***}P<0.001$ vs 0% stretch; †††$P<0.001$ for positive or negative slope; #$P<0.05$, ##$P<0.01$ shortening vs stretched sarcomeres. Detailed statistical results are presented in Tables S5 through S8.

## LDA in Single Cardiomyocytes Is Associated With Recruitment of Additional Shortening Sarcomeres

We next examined how stretch affected the uniformity of sarcomere deformation and the contribution of such effects to LDA. Cardiomyocytes were attached to glass rods and subjected to stepwise stretch in intervals corresponding to a 5% command increase in length (Figure 3A). At 20% widening of the rods, an accompanying 14.9% increase in mean SL was

observed (2.01±0.01 versus 1.75±0.02 μm at rest). As expected, cell lengthening produced an immediate and marked increase in cellular force development during 1 Hz stimulation (0.085±0.022 μN at resting length versus 0.642±0.195 μN at 20% stretch; Figure 3A, see raw data example in Figure S4 and individual data points in Figure S5). At resting length (0% stretch), attached cells exhibited heterogeneous sarcomere strain similar to observations made in cells plated on coverslips; 77±4% of sarcomeres shortened, 18±3% were stretched, and 5±2% maintained their length, despite uniform Ca2+ transients across the cell (Figure 3B and 3C). Notably, stretched sarcomeres were observed to occur at random locations between the glass rods and not exclusively near the glass rods where MyoTak attachment might cause local damage. As cells were progressively lengthened, more sarcomeres exhibited shortening during the stimulus, reaching 96±1% of sarcomeres at 20% stretch (Figure 3D). Thus, LDA includes progressive recruitment of more shortening sarcomeres.

Further analysis of sarcomere strain during LDA provided additional insight. Notably, although cell lengthening markedly increased the average SL, sarcomeres exhibiting stretch during the electrical stimulus continued to, on average, exhibit shorter resting lengths than those that shortened (Figure 3E; see Figure S6 for presentation as histograms). This observation is consistent with the view that longer sarcomeres shorten at the expense of shorter ones and that increasing SL and force production prevents sarcomeres from being abnormally stretched during electrical stimulation (see Figure S5E and S5F for correlation between proportion of shortening sarcomeres and force development). Importantly, LDA was also associated with greater magnitude contraction in shortening sarcomeres (0.12±0.01 μm in un-stretched versus 0.25±0.04 μm at full stretch), which likely reflected both increasing sarcomere force generation and reduced impedance from short sarcomeres that are stretched (Figure 3F).

**Mathematical Modeling of Sarcomere Recruitment During Rest and Stretch Conditions**

A mathematical model of sarcomere interactions was used to further investigate the heterogeneity of sarcomere strain, its underlying mechanisms, and consequences. Initial tests were performed with the dynamic model described in Methods, consisting of 3 parallel myofibrils containing 5 sarcomeres each (Figure 4A). All sarcomeres were stimulated by the Ca2+ transient shown in Figure 4B and parameterized to slightly modify the steady-state force-length dependence from the original formulation of Rice et al30 (Figure 4C). The length of a central sarcomere in the array was varied, while all others were of the average length observed in experiments (1.75 μm). In agreement with experimental observations, when the test sarcomere was shorter than average, it was effectively stretched by its neighbors—an effect that was reversed as this sarcomere was progressively lengthened (Figure 4D and 4E). Similar effects were apparent when a larger array of 30 by 50 sarcomeres was examined, with variability in SL included to mirror distributions observed in cells. These tests were performed using the steady-state version of the model and with SLs sampled randomly from a normal distribution with mean SL of 1.75 μm and 15% SD. This larger array produced similar proportions of shortening, stationary, and stretched sarcomeres as observed in experiments (Figure 4F, compare Figure 3D at resting length), with stretch again preferentially occurring when SL was short (Figure 4G). These results indicate that the modeled deformation of each sarcomere is driven by its force generation, determined by its resting length, which is counteracted by the external forces from the neighboring sarcomeres.

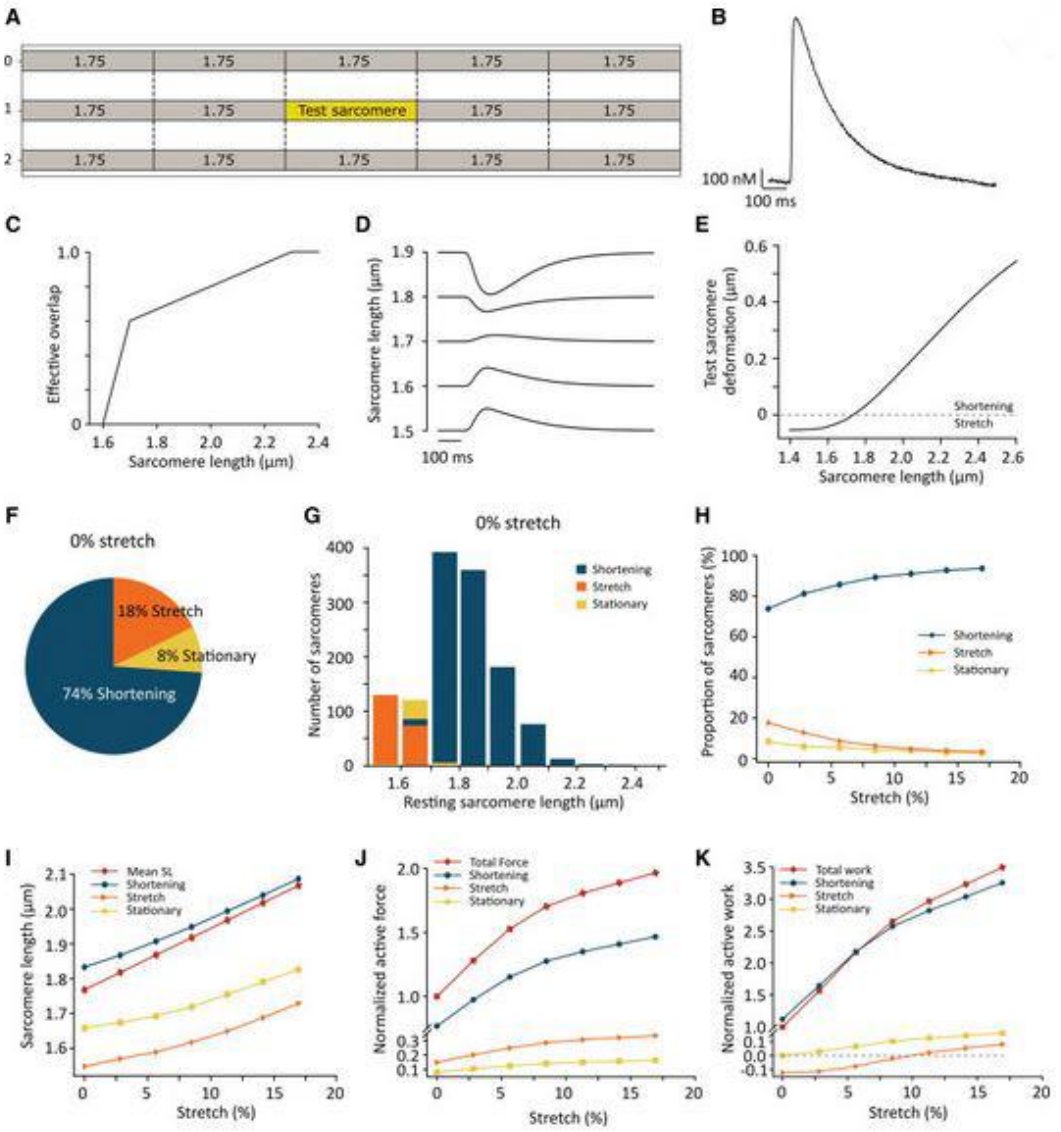


**Figure 4**. **Mathematical modeling of sarcomere recruitment during length-dependent activation. A**, Mathematical modeling of an array of 15 sarcomeres arranged in 3 myofibrils, with parallel connections via elastic springs at Z lines. Sarcomere length (SL) was varied for a central test sarcomere, while the length of other sarcomeres was maintained at 1.75 μm (the averaged resting SL in experimental data). **B**, Sarcomeres were stimulated by a representative experimental Ca2+ transient. **C**, The steady-state force-length dependence derived from Rice et al,30 quantifying the region where a single thin filament overlaps with the crossbridge containing region of the thick filament. **D** and **E**, Modeled strain of test sarcomere in **A** as a function of resting SL. **F**, An expanded array of 150 sarcomeres arranged in 30 myofibrils was used to include the SL variability observed experimentally. The SLs were randomly generated by using a normal distribution with mean of 1.75 μm and 15% SD (Figure 3D; 0% stretch). Proportions of shortening, stretched, and stationary sarcomeres. **G**, Distribution of resting SL values for each type of strain. **H**, Stepwise lengthening of the sarcomere array progressively increased the number of shortening sarcomeres. **I**, Corresponding changes in SL. **J**, Active sarcomere force production. **K**, Stepwise recruitment of shortening sarcomeres increased overall work performance as less negative work was performed by stretched sarcomeres.

To examine the effects of cell stretch, the larger modeled sarcomere array was lengthened in a stepwise manner, with simultaneous interrogation of sarcomere strain and force generation. The results broadly confirmed experimental findings that fiber lengthening enables progressive recruitment of increasing numbers of shortening sarcomeres (Figure 4H). Fiber

lengthening increased SL (Figure 4I) and force production (Figure 4J) in all sarcomeres, regardless of whether they were initially shortening, stationary, or stretched at resting length. However, the stretched sarcomere group exhibited the largest increase in active force (223%), due to the fact that the force-length relationship is steeper at short SLs. Thus, there was a modest steepening of the overall force-length relationship beyond that generated by the pool of sarcomeres that initially shortened (127% force increase; Figure 4J). Critically, the augmenting force production in short sarcomeres allowed them to overcome the stretching effects of their longer neighbors and exhibit shortening. This effect increased overall contractile efficiency during cell lengthening, as estimated by work performance (Figure 4K). Indeed, the negative, wasted work lost to stretched sarcomeres was reversed as these sarcomeres were sufficiently lengthened to enable their shortening. Thus, less force was dissipated at longer lengths, and the overall work-length relationship was steepened, crossing that of the shortening sarcomere group (Figure 4K). A schematic illustrating the critical role of SL in controlling the recruitment of shortening sarcomeres during cell lengthening is presented in Figure 5.

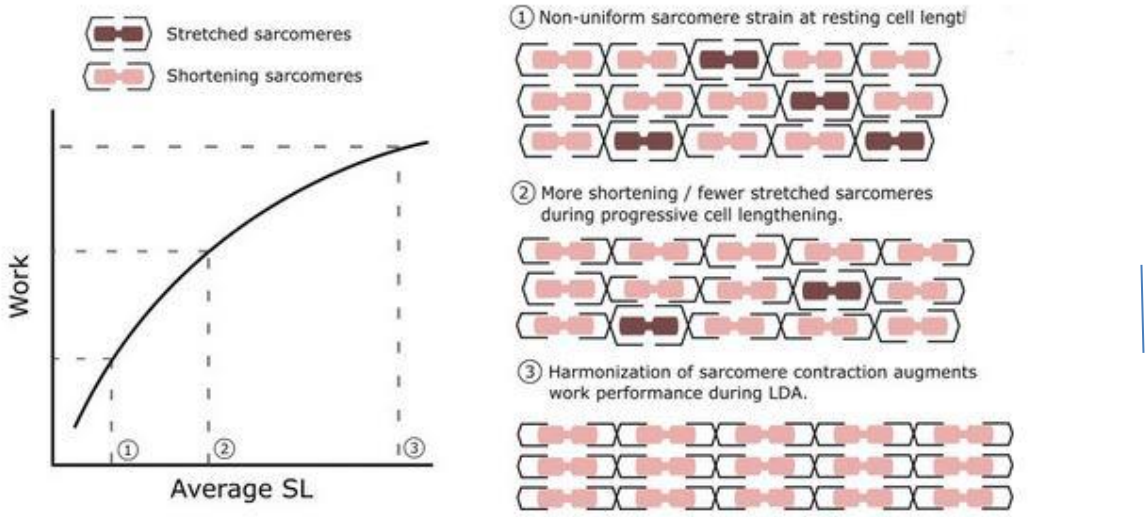


**Figure 5**. **Cell lengthening harmonizes sarcomere strain patterns, augmenting work performance.** Schematic overview of findings, showing the presence of both shortening and stretched sarcomeres within myofibrils. Stretched sarcomeres are illustrated with shorter sarcomere length. Lower likelihood of crossbridge formation at these sarcomeres may reflect larger interfilament lattice spacing (illustrated) or lower stretch-dependent activation of the thin and thick filaments. Progressive stretch of the myofibril increases the fraction of shortening sarcomeres, as lengthening the shortest sarcomeres recruits their active force generation (to overcome the stretching effects of their longer neighbors). Increasing sarcomere recruitment during cell lengthening augments overall contractile efficiency, as less wasted (negative) work is performed.

## Titin Controls Variability in SL, Sarcomere Recruitment, and Work Performance

Since our observations indicate that SL is a key determinant of the recruitment of shortening sarcomeres, we investigated the underlying causes. First, we examined whether variable SL might reflect regional differences in resting Ca2+ levels across the cell. To this end, cardiomyocytes were permeabilized either by ionophores or saponin to normalize intracellular

Ca2+. In the presence of 0 mM extracellular Ca2+, permeabilization caused an expected increase in SL but no change in its variability across the cell (Figure S7).

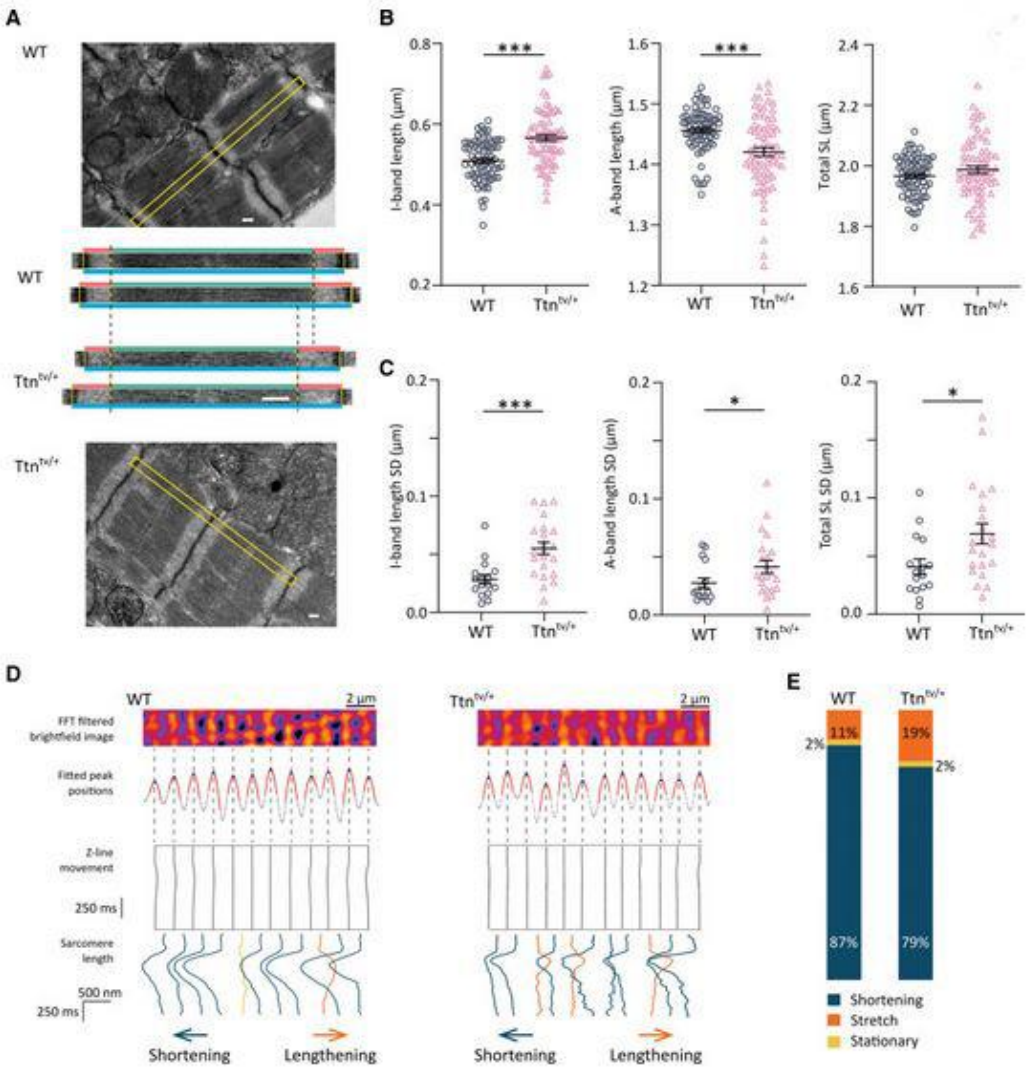


**Figure 6**. **Titin regulates sarcomere dimensions and intersarcomere dynamics. A**, Representative micrographs from fixed WT (wild type) and Ttntv/+ mouse myocardium. Enlargements of 2 neighboring sarcomeres indicate the length of the I band (red bar), A band (green), and overall sarcomere length (blue) and highlight the variability of these dimensions. Scale bars, 0.2 µm. **B**, Mean I band, A band, and total sarcomere lengths (±SEM). **C**, Variability in sarcomere dimensions, calculated as SD within each image, presented as mean± SEM. nsarcomeres: WT, 71 from 3 hearts; Ttntv/+, 72 from 3 hearts. **D**, Sarcomere tracking experiments in Ttntv/+ cells revealed fewer shortening and more stretched sarcomeres than in WT (dark blue traces, shortening; orange traces, stretched). **E**, Proportions of shortening, stretched, and stationary sarcomeres. nsarcomeres: WT, 260 from 23 cells, 3 hearts; Ttntv/+, 248 from 19 cells, 3 hearts. Statistical methods: (**B** and **C**) Mann-Whitney *U* test; (**E**) $\chi 2$ test (proportion stretched sarcomeres in WT vs TTNtv/+, $P$=0.00396). $P$<0.05 was considered significant (*$P$<0.05, ***$P$<0.001). Detailed statistical results are shown in Table S9.

An alternative explanation is that titin, which critically sets sarcomere dimensions,[31,32] centers the A band in the contracting sarcomere[21] and preserves Z-line and A-band alignment,[33] regulates the uniformity of sarcomere strain. To investigate this hypothesis, we examined titin mutant (Ttntv/+) mice that exhibit haploinsufficiency.[26] Overall sarcomere alignment was observed to be unaltered in light microscopy images of Ttntv/+ and WT (wild

type) control myocytes (Figure S8A and S8B). However, more detailed analysis of sarcomeric structure by electron microscopy revealed key differences (Figure 6A). Specifically, we observed that although overall SL was similar, myocytes isolated from mutant mice exhibited longer I-band length and shorter A band than WT (Figure 6B), a trend that was observed across the range of measured SLs (Figure S8C and S8D). These findings are in agreement with previous reports that titin is critical for normal myosin filament assembly31,32 and maintenance during contraction.33 Interestingly, I-band and A-band lengths were also observed to be more variable in Ttntv/+ compared with WT, leading to significantly greater variability in overall SL, as measured both in electron microscopy (EM) images (Figure 6C) and light microscopy images of living cells (Figure S9; F test, $P$=0.038). Greater SL variability in Ttntv/+ was, in turn, linked to a significant increase in the proportion of stretched sarcomeres (19%) compared with WT cells (11%; Figure 6D and 6E; $\chi 2$ test, $P$=0.023). The resting length of stretched sarcomeres was similar in Ttntv/+ and WT cells (SL, 1.75±0.03 versus 1.71±0.03 µm, respectively; $P$=0.321). These findings are consistent with an important role of titin in regulating both sarcomere dimensions and intersarcomere strain patterns across the cell.

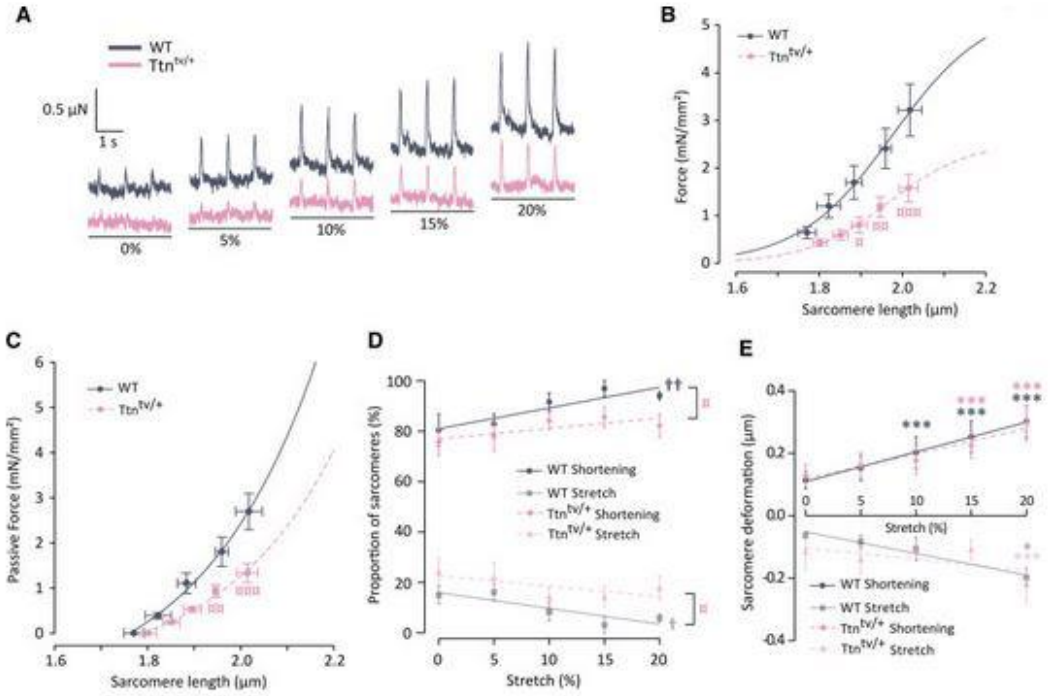


**Figure 7**. **During lengthening, Ttntv/+ cardiomyocytes exhibit diminished length-dependent activation and passive stiffness and greater non-uniformity of sarcomere strain. A**, Representative developed force recordings for WT (wild type) and Ttntv/+ cardiomyocytes during stepwise stretch experiments, with mean measurements presented in **B** (values normalized to cell width). ncells, hearts: WT: 5, 3; Ttntv/+: 6, 3. **C**, Mean passive force measurements for the same cells, assessed as basal force at each step of stretch. **D**, Proportions of shortening and stretched sarcomeres. **E**, Magnitude of deformation for shortening and stretched sarcomeres. $n_{sarcomeres}$: WT: 0% stretch, 103; 5% stretch, 105; 10% stretch, 99; 15% stretch, 106; 20% stretch, 94, from 5 cells, 3 hearts; Ttntv/+: 0% stretch, 99; 5% stretch, 107; 10% stretch, 120; 15% stretch, 117; 20% stretch, 115, from 6 cells, 3 hearts. Data are presented as mean ± SEM with sigmoidal curve fitting (**B**), exponential curve fitting (**C**), or linear regression (**D** and **E**). Statistic methods: (**B** and **C**) 2-way repeated measures ANOVA; (**D**) linear mixed model; (**E**) Kruskal-Wallis test for within-group comparisons, Mann-Whitney *U* test for between-group comparisons. $P$<0.05 was considered significant. For WT vs Ttntv/+, ¤$P$<0.05, ¤¤$P$<0.01, ¤¤¤$P$<0.001, †$P$<0.05, ††$P$<0.01 for positive or negative slope. For presented within group comparisons, *$P$<0.05, ***$P$<0.001. Detailed statistical results for **B** through **E** are presented in Tables S10 through S14.

We next affixed cardiomyocytes to glass rods to examine the consequences of titin haploinsufficiency for sarcomere strain and force development during cell lengthening. In comparison with WT controls, Ttntv/+ mouse cardiomyocytes exhibited reduced force generation, particularly at long SLs (Figure 7A and 7B; see Figure S10 for individual data points). In keeping with lowered titin expression, Ttntv/+ cells also exhibited lowered passive stiffness, as measured by the increase in resting force induced by each stepwise lengthening of the cell (Figure 7C). Importantly, the proportion of sarcomeres that was stretched during each electrical stimulation remained higher in Ttntv/+ cells compared with WT, even as the cells were lengthened (Figure 7D). Thus, at 20% stretch, although nearly all sarcomeres (94%) were recruited to shorten in WT, only 82% were observed to shorten in Ttntv/+. The magnitude of sarcomere deformation (shortening or stretch) was similar in WT and Ttntv/+ across the range of cell lengths (Figure 7E). These results indicate that titin haploinsufficiency is linked to reductions in both sarcomere recruitment and LDA.

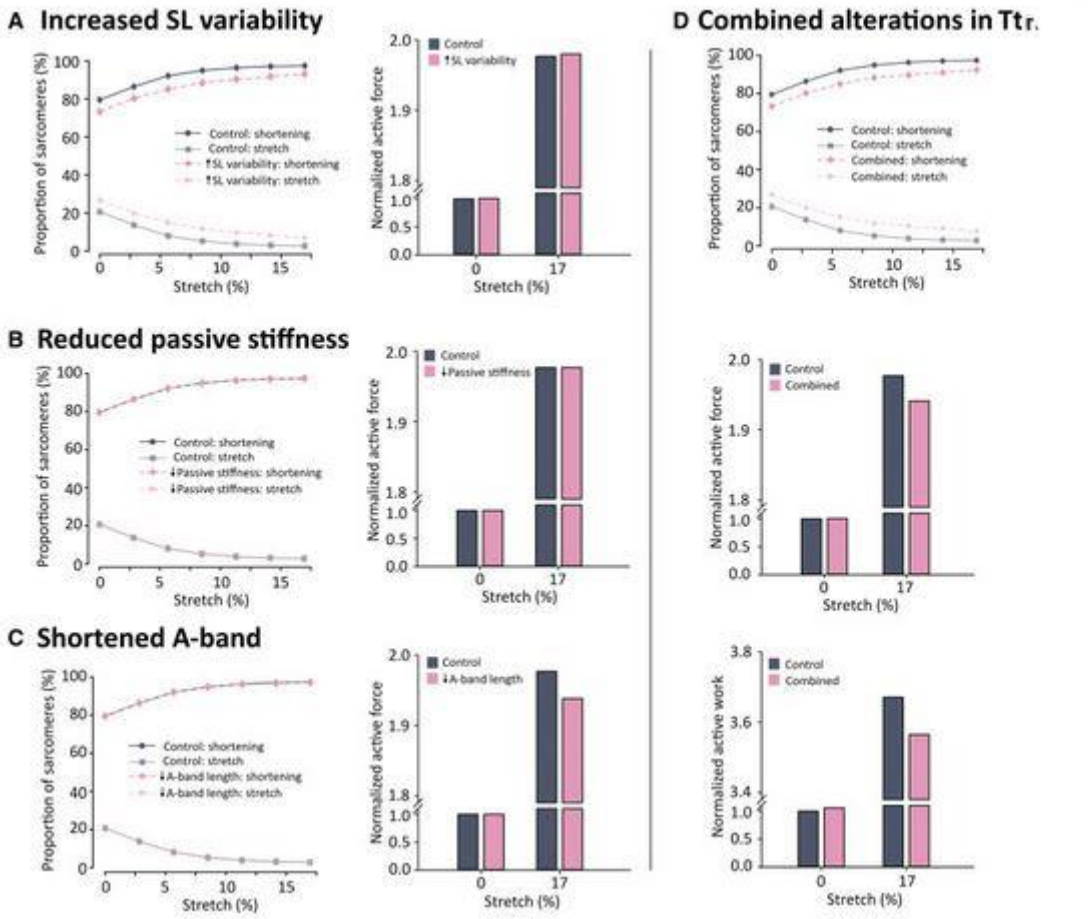


**Figure 8**. **Increased non-uniformity of sarcomere strain and lowered force production culminate in impaired work performance in TTNtv/+.** Changes in TTNtv/+ cardiomyocytes observed experimentally (Figures 6 and 7) were incorporated in the modeled array of 1500 sarcomeres to examine effects of stretch on the uniformity of sarcomere strain, force production, and work performance. Changes included (**A**) increasing sarcomere length variability by 4%, (**B**) reducing passive stiffness by 50%, and (**C**) shortening the A band by 3%. Combining these alterations (**D**) resulted in a higher proportion of stretched sarcomeres and lowered force and work production following stretch. Similar results were obtained when changes in passive stiffness were excluded (Figure S11).

Finally, we examined whether the experimental measurements in Ttntv/+ cardiomyocytes could be reproduced by the deterministic mathematical model. We specifically interrogated the effect of 3 observed changes in these cells: (1) increased SL variability, (2) decreased passive force, and (3) decreased length of the A band, which is expected to reduce the number of myosin heads available for force generation. Incorporating the observed increase in SL variability in the model successfully reproduced lower sarcomere recruitment (fewer shortening sarcomeres) across a range of cell lengths (Figure 8A, left). However, there was little effect of this change on active force generation (Figure 8A, right), since the proportion of shortening sarcomeres increased in parallel in the 2 conditions. In contrast, using experimental measurements to decrease the passive stiffness in the model had little discernible effect on sarcomere recruitment or force generation (Figure 8B). Decreasing the length of the A band, and thus the number of myosin heads, also did not alter the proportion of shortening sarcomeres (Figure 8C, left). However, as in cell experiments, force production was reduced when the sarcomere array was lengthened, as the shorter A band resulted in fewer crossbridges with the thin filaments (Figure 8C, right). When the 3 alterations were made in combination, the model reproduced the lowered sarcomere recruitment and LDA observed experimentally in Ttntv/+ cardiomyocytes (Figure 8D). Overall work performance was also reduced, owing to both lowered force production and a higher fraction of stretched sarcomeres performing negative work (Figure 8D, bottom). Similar observations were made when only increased SL variability and decreased A-band length were combined in the model (ie, without changes in passive stiffness; Figure S11). These findings provide an explanation for impaired cardiomyocyte function resulting from titin truncating mutations.

# Discussion

Current dogma has generally assumed that sarcomeres contract uniformly across healthy cardiomyocytes. Our present results dispute this view, showing that in un-stretched cells, there is in fact marked heterogeneity of sarcomere strain during electrical stimulation. Specifically, using 2 different imaging techniques, we observed that while ≈85% of sarcomeres shortened during the electrical stimulus, ≈10% were stretched, and a small remainder of sarcomeres stayed stationary. These distinct patterns of sarcomere strain were linked to differences in resting SL, and mathematical modeling confirmed that lower force production in short sarcomeres can cause them to be stretched by their longer neighbors. Cell stretch was observed to harmonize sarcomere strain in healthy cells, as an increase in average SL from ≈1.75 to 2 μm was accompanied by nearly full sarcomere recruitment to shorten during the electrical stimulus. Thus, LDA includes a previously unrecognized increase in work performance, as recruited sarcomeres begin to produce positive instead of negative work. Based on these findings, we propose a mechanistic model as schematically illustrated in Figure 5.

Why does this harmonization of sarcomere strain occur as the cell is lengthened? Our mathematical modeling analyses show that variability in SL is critical, since it provides a pool of short sarcomeres that produce sufficiently low force to allow their stretch in the resting state. Indeed, the modeled relationship between effective myofilament overlap, a surrogate for force development, and SL (Figure 4C) predicts that longer, shortening sarcomeres produce 56% more force than their shorter, stretched counterparts (0.653 versus 0.420, using mean experimental SLs in Figure 2D). Due to the steep nature of the force-SL relationship at short

SLs, short sarcomeres that previously were stretched become contractile when their sharply increasing active force production results in a more balanced tug of war with their longer neighbors. It is important to note that the steep portion of the force-length relationship used in the mathematical model occurred at SLs <1.7 μm (Figure 4C), while the mean SL recorded experimentally in resting cells was ≈1.75 μm. Thus, the steepest portion of the cell's overall force-length relationship is in fact absent in real cardiomyocytes during stretch (Figures 3A and 7B). Nevertheless, we did observe many individual sarcomeres as short as those in the steepest range of the force-length relationship (≈1.6 μm) in resting cardiomyocytes, and this pool of short sarcomeres gradually disappeared as the cell was lengthened (Figure S5C). Recruitment of previously stretched sarcomeres to shorten was manifested as a steepening of the cell's work-length relationship (Figure 4K).

What then controls variability in SL? In the second part of our study, we proposed a central role of titin, since previous work has indicated that this protein regulates sarcomere geometry,31,32 and eliminating titin stiffness by acute cleavage of I-band titin causes disruption of the contracting sarcomere.33 Indeed, our electron microscopy analyses revealed considerable variability within the I band of healthy cells (Figure 6A and 6B), where dimensions are critically set by titin. In an un-stretched cell, slackened titin allows a greater range of movement within this region. We expect accompanying irregularity in A-band radial force and variability in lattice spacing or strain-induced activation of the myofilaments (recruitment of myosin heads to the on state, MyBP-C binding to thin filaments, altered troponin configuration).15,17,21,22,34 Such effects would in turn lead to variable efficiency of force production between sarcomeres in the un-stretched state (Figure 5). To further investigate the role of titin in controlling sarcomere dimensions and strain, we examined cardiomyocytes with lowered titin expression due to haploinsufficiency.26 In $TTN^{tv/+}$ cells, we observed even greater variability in I-band length and overall SL (Figure 6A and 6C) and an even larger proportion of stretched sarcomeres during electrical stimulation (Figure 6D and 6E). Stretching $TTN^{tv/+}$ cells resulted in recruitment of additional shortening sarcomeres, but the proportion of stretched sarcomeres still remained higher than values observed in WT (Figures 7D and 8A). Thus, our data support that increased non-uniformity of sarcomere strain in $TTN^{tv/+}$ cells is a novel mechanism underlying impaired cardiac performance in individuals with these mutations.

Beyond titin's role in controlling variability of SL, our observations support an emerging view that titin levels critically regulate myofilament assembly.31,32 $TTN^{tv/+}$ cells exhibited a shorter A band (Figure 6A and 6B) consistent with a decreased number of myosin heads available to form crossbridges. Mirroring experimental observations (Figure 7A and 7B), mathematical modeling showed that the shorter A band resulted in less robust overlap of thick and thin filaments during stretch and impaired force development (Figure 8C). Thus, during LDA, impaired work performance in $TTN^{tv/+}$ stems from 2 sources; a decreased length of the A band, which reduces force development, and more variable length of the I band, which promotes non-homogeneity of sarcomere strain (Figure 8D).

Although our results show that the cell's titin content coordinates strain patterns between sarcomeres, we had suspected that the protein's stiffness might also play a role. However, mathematical modeling showed that an observed reduction in passive stiffness in $TTN^{tv/+}$ had no effect on either sarcomere strain or force production (Figure 8B). However, local differences in titin isoforms may be relevant. In healthy rats and mice, the stiff N2B isoform predominates, while the more compliant N2BA isoform accounts for 5% to 15% of expressed titin.35,36 It seems plausible that the longer, extensible I band of N2BA may allow more

variability in SL where it is present and that the shortest sarcomeres that exhibit stretch in healthy cells at resting length could be those that express N2BA. As the subject of future work, investigation of this hypothesis is expected to be hampered by a current lack of isoform-specific antibodies and difficulties in quantifying regional differences in phosphorylation and oxidation.

A key question that arises from the current work is whether recruitment of additional shortening sarcomeres contributes to the Frank-Starling mechanism in an in vivo setting. Central to this understanding is insight into the range of SL in intact tissue, a point that has been somewhat controversial and difficult to investigate. To address this issue on a preliminary basis, we presently investigated SL variability in intact, living ventricular tissue by confocal microscopy (Figure S12). We observed that the SD of these SL measurements (0.182) was actually somewhat larger than measurements made in isolated cells (0.123 from t tubule–tracking experiments and 0.083 from Z-line–tracking experiments). Thus, despite the presence of the extracellular matrix and intercellular connections, these data support that sarcomere in-homogeneities are present in the intact, living ventricle. We found that mean SL was ≈1.89 μm in intact tissue. This value is in close agreement with previous reports of diastolic SL in the in vivo mouse heart[37,38] and in explanted, Langendorff-perfused rat hearts.[39] At this SL, we observed that a significant proportion of sarcomeres (11.4%) is stretched in isolated cells (calculated from regression line in Figure 3D and 3E). Thus, at least in small rodents under low preload conditions, it appears that sarcomeres likely remain available for recruitment during activation of the Frank-Starling mechanism. Such effects may be particularly relevant in disease states such as the post-infarction heart, where cardiomyocytes positioned proximal to a scar may experience reduced preload. Future work should be aimed at examining homogeneity of sarcomere function in the in vivo heart, to quantify how harmonization of sarcomere strain contributes to the Frank-Starling mechanism in both health and disease.

It is interesting to consider why the presently described changes in sarcomere strain during LDA have not been previously reported in cardiomyocytes. Indeed, even the concept of non-homogeneous sarcomere function appears to have been overlooked by some investigators, who have examined sarcomere dynamics with Fourier transforms to assess average changes in Z-line positions[40,41] or simply recorded overall cell length. Furthermore, previous efforts to track Z lines have generally not sought to reduce the noise of the individual sarcomere signals or have used too low frame rates to adequately detect changes in length during the contraction cycle. However, 2 previous studies by the Fukuda group have reported heterogeneous sarcomere strain in neonatal cardiomyocytes,[42,43] where dyssynchronous $Ca^{2+}$ release due to a lack of t tubules is expected to be a contributing factor.[44] Heterogeneous sarcomere strain has also been noted on occasion in adult myocytes during systole,[45–48] diastole,[49] and during $Ca^{2+}$ sparks and waves.[50,51] Finally, it should be noted that our findings conceptually resemble observations of nonhomogeneous function in the whole heart, including reports of positive strain occurring proximal to an infarction[52] and during dyssynchronous heart failure.[53] In such situations, it is believed that strongly contracting segments shorten at the expense of weaker regions that are stretched. Thus, our present results are broadly similar to observations made previously in the intact heart but at a smaller scale within cardiomyocytes.

Interestingly, sarcomeric non-uniformities have also been reported in skeletal muscle, where it has similarly been suggested that some sarcomeres may be stretched by their strongly contracting neighbors,[54] despite similar local $Ca^{2+}$ signals.[55,56] However, here, an important distinction should be made from the mechanisms presently described, since even

resting skeletal muscle operates at much longer SL than cardiac muscle (Figure S13A and S13B). Our experimental measurements (Figure 2D) suggest that there is a threshold SL ≈1.8 μm, beyond which force generation is sufficient to ensure sarcomere shortening. Although we observed considerable variability in SL in skeletal muscle, we did not observe any sarcomeres shorter than 1.8 μm (Figure S13B), and including SL measurements in the mathematical model showed uniform sarcomere strain, as all sarcomeres shortened (Figure S13C). Thus, our observations of nonuniform sarcomere strain at rest, and recruitment of contracting sarcomeres during stretch, appear to be most relevant to cardiomyocytes.

Some limitations of our work should be noted. Our first approach to tracking sarcomere function relied on confocal t-tubule imaging as an estimate of Z-line positions. Although t tubules are certainly localized nearby Z lines, recent work has indicated that they deform during each contraction/relaxation cycle.29 Nevertheless, deviations of the t-tubule fluorescent signal from the true Z-line position are expected to be small and likely within the calculated sensitivity for detecting sarcomere movement. Our second sarcomere tracking technique had the advantage that Z lines were directly visualized. However, since this technique used wide-field imaging, a thicker axial section of the cell was tracked. It is thus possible that tilting of Z lines within the axial plane may have affected demarcation of the sarcomere ends. Despite these shortcomings, the 2 techniques revealed remarkably similar non-uniformity of sarcomere dynamics, including the observed proportions of shortening, stretched, and stationary sarcomeres and their respective differences in resting SL. Thus, we believe that these complementary approaches have provided robust insight into the function of individual sarcomeres in isolated cardiomyocytes. However, our study has not included an examination of the many factors other than SL that are expected to contribute to local sarcomere strain, including posttranslational modifications and activation states of the thick and thin filaments or local differences in myofilament Ca2+ sensitivity. Indeed, although we observed that mean SL of stretched sarcomeres is on average shorter than in shortening sarcomeres, there is overlap of these distributions (Figures 1D and 2D). Thus, our present work represents only a first step in understanding local differences in sarcomere force generation and strain. Finally, it should be noted that none of our study's experiments included cells or tissue from animals of each sex. This shortcoming reflects the demanding nature of the methods used, which precluded the possibility to record from sufficiently large sample sizes to allow analysis of sex as a biological variable.

In conclusion, our present findings indicate that in the un-stretched state, cardiomyocytes exhibit nonhomogeneous sarcomere strain during electrical stimulation. This non-uniformity results from differences in resting SL across the cell, as short, weakly contracting sarcomeres are stretched by their longer neighbors. Upon cell lengthening, augmenting force production in these shorter sarcomeres enables their gradual recruitment. The resulting harmonization of sarcomere shortening along the cell increases the efficiency of contraction, as less wasted work is performed by stretched sarcomeres. By tuning SL, titin regulates intersarcomere dynamics. In cardiomyocytes with titin haploinsufficiency mutation, lowered titin levels yield more variability in I-band length, and a greater proportion of stretched sarcomeres, while a shorter A band reduces force generation during LDA. In combination, we show that these changes impair work performance in $TTN^{tv/+}$ myocytes, identifying a novel mechanism for impaired contractility in this condition.

**Affiliations**

Institute for Experimental Medical Research, Oslo University Hospital and University of Oslo, Norway (J.L., Y.H., M.L., M.R., T.R.K., M.F., P.A.N., I.E.S., O.M.S., I.G.L., W.E.L.). KG Jebsen Center for Cardiac Research, University of Oslo, Norway (J.L., Y.H., M.L., M.R., T.R.K., M.F., I.E.S., O.M.S., I.G.L., W.E.L.). Simula Research Laboratory, Lysaker, Norway (J.S.). DNV, Høvik, Norway (L.Y.). Institute of Physiology II, University of Münster, Germany (A.U., W.A.L.). Department of Physiology and Pharmacology, Karolinska Institutet, Stockholm, Sweden (E.S.A., M.K., J.T.L.). Department of Physiology and Biophysics, University of Illinois at Chicago (P.P.d.T.). Phymedexp, Université de Montpellier, INSERM, CNRS, France (P.P.d.T.).

**Acknowledgments**

The authors thank the Section for Comparative Medicine at Oslo University Hospital Ullevål for expert animal care. They are also grateful for statistical assistance provided by Luigi A. Maglanoc in the Information Technology Department at the University of Oslo.

**Sources of Funding**

This work was financially supported by the European Union Horizon 2020 Research and Innovation Progamme (consolidator grant, W.E. Louch; under grant agreement number 647714), the Norwegian Research Council under project number 287395 (W.E. Louch), and The Norwegian Association for Public Health (J. Li and W.E. Louch).

**Disclosures**

None.

# References

1. Huxley HE. Structural difference between resting and rigor muscle - evidence from intensity changes in low-angle equatorial X-ray diagram. J Mol Biol. 1968;37:507–520. doi: 10.1016/0022-2836(68)90118-6 - PubMed
2. Mansson A, Usaj M, Moretto L, Rassier DE. Do actomyosin single-molecule mechanics data predict mechanics of contracting muscle? Int J Mol Sci. 2018;19:1863. doi: 10.3390/ijms19071863 - PMC - PubMed
3. Flucher BE, FranziniArmstrong C. Formation of junctions involved in excitation-contraction coupling in skeletal and cardiac muscle. P Natl Acad Sci USA. 1996;93:8101–8106. doi: 10.1073/pnas.93.15.8101 - PMC - PubMed
4. Lehman W, Hatch V, Korman V, Rosol M, Thomas L, Maytum R, Geeves MA, Van Eyk JE, Tobacman LS, Craig R. Tropomyosin and actin isoforms modulate the localization of tropomyosin strands on actin filaments. J Mol Biol. 2000;302:593–606. doi: 10.1006/jmbi.2000.4080 - PubMed
5. Herzberg O, Moult J, James MNG. A model for the Ca2+-induced conformational transition of troponin-C - a trigger for muscle-contraction. J Biol Chem. 1986;261:2638–2644. - PubMed

6. Mckillop DFA, Geeves MA. Regulation of the interaction between actin and myosin subfragment-1 - evidence for 3 states of the thin filament. Biophys J. 1993;65:693–701. doi: 10.1016/S0006-3495(93)81110-X - PMC - PubMed
7. de Tombe PP, Mateja RD, Tachampa K, Ait Mou Y, Farman GP, Irving TC. Myofilament length dependent activation. J Mol Cell Cardiol. 2010;48:851–858. doi: 10.1016/j.yjmcc.2009.12.017 - PMC - PubMed
8. Fukuda N, Terui T, Ohtsuki I, Ishiwata S, Kurihara S. Titin and troponin: central players in the frank-starling mechanism of the heart. Curr Cardiol Rev. 2009;5:119–124. doi: 10.2174/157340309788166714 - PMC - PubMed
9. Hibberd MG, Jewell BR. Calcium-dependent and length-dependent force production in rat ventricular muscle. J Physiol-London. 1982;329:527–540. doi: 10.1113/jphysiol.1982.sp014317 - PMC - PubMed
10. Terkeurs HEDJ, Rijnsburger WH, Vanheuningen R, Nagelsmit MJ. Tension development and sarcomere-length in rat cardiac trabeculae - evidence of length-dependent activation. Circ Res. 1980;46:703–714. doi: 10.1161/01.Res.46.5.703 - PubMed
11. Zhang X, Kampourakis T, Yan Z, Sevrieva I, Irving M, Sun YB. Distinct contributions of the thin and thick filaments to length-dependent activation in heart muscle. Elife. 2017;6:e24081. doi: 10.7554/eLife.24081 - PMC - PubMed
12. Kentish JC, Terkeurs HEDJ, Ricciardi L, Bucx JJJ, Noble MIM. Comparison between the sarcomere length-force relations of intact and skinned trabeculae from rat right ventricle - influence of calcium concentrations on these relations. Circ Res. 1986;58:755–768. doi: 10.1161/01.Res.58.6.755 - PubMed
13. Mcdonald KS, Moss RL. Osmotic compression of single cardiac myocytes eliminates the reduction in Ca2+ sensitivity of tension at short sarcomere-length. Circ Res. 1995;77:199–205. doi: 10.1161/01.res.77.1.199 - PubMed
14. Konhilas JP, Irving TC, de Tombe PP. Myofilament calcium sensitivity in skinned rat cardiac trabeculae - role of interfilament spacing. Circ Res. 2002;90:59–65. doi: 10.1161/hh0102.102269 - PubMed
15. Ait-Mou Y, Hsu K, Farman GP, Kumar M, Greaser ML, Irving TC, de Tombe PP. Titin strain contributes to the Frank-Starling law of the heart by structural rearrangements of both thin- and thick-filament proteins. Proc Natl Acad Sci USA. 2016;113:2306–2311. doi: 10.1073/pnas.1516732113 - PMC - PubMed
16. Kampourakis T, Sun YB, Irving M. Myosin light chain phosphorylation enhances contraction of heart muscle via structural changes in both thick and thin filaments. Proc Natl Acad Sci USA. 2016;113:E3039–E3047. doi: 10.1073/pnas.1602776113 - PMC - PubMed
17. Campbell KS, Janssen PML, Campbell SG. Force-dependent recruitment from the myosin off state contributes to length-dependent activation. Biophys J. 2018;115:543–553. doi: 10.1016/j.bpj.2018.07.006 - PMC - PubMed
18. Linari M, Brunello E, Reconditi M, Fusi L, Caremani M, Narayanan T, Piazzesi G, Lombardi V, Irving M. Force generation by skeletal muscle is controlled by mechanosensing in myosin filaments. Nature. 2015;528:276–279. doi: 10.1038/nature15727 - PubMed
19. Reconditi M, Caremani M, Pinzauti F, Powers JD, Narayanan T, Stienen GJM, Linari M, Lombardi V, Piazzesi G. Myosin filament activation in the heart is tuned to the mechanical task. Proc Natl Acad Sci USA. 2017;114:3240–3245. doi: 10.1073/pnas.1619484114 - PMC - PubMed

20. Pfuhl M, Gautel M. Structure, interactions and function of the N-terminus of cardiac myosin binding protein C (MyBP-C): who does what, with what, and to whom? J Muscle Res Cell Motil. 2012;33:83–94. doi: 10.1007/s10974-012-9291-z - PubMed
21. Linke WA. Titin gene and protein functions in passive and active muscle. Annu Rev Physiol. 2018;80:389–411. doi: 10.1146/annurev-physiol-021317-121234 - PubMed
22. Methawasin M, Hutchinson KR, Lee EJ, Smith JE, Saripalli C, Hidalgo CG, Ottenheijm CAC, Granzier H. Experimentally increasing titin compliance in a novel mouse model attenuates the Frank-Starling mechanism but has a beneficial effect on diastole. Circulation. 2014;129:1924–1936. doi: 10.1161/CIRCULATIONAHA.113.005610 - PMC - PubMed
23. Fukuda N, Sasaki D, Ishiwata S, Kurihara S. Length dependence of tension generation in rat skinned cardiac muscle - role of titin in the Frank-Starling mechanism of the heart. Circulation. 2001;104:1639–1645. doi: 10.1161/hc3901.095898 - PubMed
24. Li KL, Methawasin M, Tanner BCW, Granzier HL, Solaro RJ, Dong WJ. Sarcomere length-dependent effects on Ca2+-troponin regulation in myocardium expressing compliant titin. J Gen Physiol. 2019;151:30–41. doi: 10.1085/jgp.201812218 - PMC - PubMed
25. Hessel AL, Ma W, Mazara N, Rice PE, Nissen D, Gong H, Kuehn M, Irving T, Linke WA. Titin force in muscle cells alters lattice order, thick and thin filament protein formation. Proc Natl Acad Sci USA. 2022;119:e2209441119. doi: 10.1073/pnas.2209441119 - PMC - PubMed
26. Garcia-Pavia P, Kim Y, Restrepo-Cordoba MA, Lunde IG, Wakimoto H, Smith AM, Toepfer CN, Getz K, Gorham J, Patel P, et al. . Genetic variants associated with cancer therapy-induced cardiomyopathy. Circulation. 2019;140:31–41. doi: 10.1161/CIRCULATIONAHA.118.037934 - PMC - PubMed
27. Fomin A, Gartner A, Cyganek L, Tiburcy M, Tuleta I, Wellers L, Folsche L, Hobbach AJ, von Frieling-Salewsky M, Unger A, et al. . Truncated titin proteins and titin haploinsufficiency are targets for functional recovery in human cardiomyopathy due to TTN mutations. Sci Transl Med. 2021;13:eabd3079. doi: 10.1126/scitranslmed.abd3079 - PubMed
28. Stroeks S, Lunde IG, Hellebrekers D, Claes GRF, Wakimoto H, Gorham J, Krapels IPC, Vanhoutte EK, van den Wijngaard A, Henkens M, et al. . Prevalence and clinical consequences of multiple pathogenic variants in dilated cardiomyopathy. Circ Genom Precis Med. 2023;16:e003788. doi: 10.1161/CIRCGEN.122.003788 - PubMed
29. Rog-Zielinska EA, Scardigli M, Peyronnet R, Zgierski-Johnston CM, Greiner J, Madl J, O'Toole ET, Morphew M, Hoenger A, Sacconi L, et al. . Beat-by-beat cardiomyocyte t-tubule deformation drives tubular content exchange. Circ Res. 2021;128:203–215. doi: 10.1161/CIRCRESAHA.120.317266 - PMC - PubMed
30. Rice JJ, Wang F, Bers DM, de Tombe PP. Approximate model of cooperative activation and crossbridge cycling in cardiac muscle using ordinary differential equations. Biophys J. 2008;95:2368–2390. doi: 10.1529/biophysj.107.119487 - PMC - PubMed
31. Granzier H, Tonino P, Kiss B, Strom J, Smith J, Methawasin M, Kolb J. The giant protein titin regulates the length of the striated muscle thick filament-titin rules. Biophys J. 2018;114:496a–496a. doi: 10.1016/j.bpj.2017.11.2718 - PMC - PubMed

32. Bennett P, Rees M, Gautel M. The axial alignment of titin on the muscle thick filament supports its role as a molecular ruler. J Mol Biol. 2020;432:4815–4829. doi: 10.1016/j.jmb.2020.06.025 - PMC - PubMed
33. Li Y, Hessel AL, Unger A, Ing D, Recker J, Koser F, Freundt JK, Linke WA. Graded titin cleavage progressively reduces tension and uncovers the source of A-band stability in contracting muscle. Elife. 2020;9:e64107. doi: 10.7554/eLife.64107 - PMC - PubMed
34. Fukuda N, Wu Y, Farman G, Irving TC, Granzier H. Titin isoform variance and length dependence of activation in skinned bovine cardiac muscle. J Physiol. 2003;553:147–154. doi: 10.1113/jphysiol.2003.049759 - PMC - PubMed
35. Warren CM, Krzesinski PR, Campbell KS, Moss RL, Greaser ML. Titin isoform changes in rat myocardium during development. Mech Develop. 2004;121:1301–1312. doi: 10.1016/j.mod.2004.07.003 - PubMed
36. Cazorla O, Freiburg A, Helmes M, Centner T, McNabb M, Wu Y, Trombitas K, Labeit S, Granzier H. Differential expression of cardiac titin isoforms and modulation of cellular stiffness. Circ Res. 2000;86:59–67. doi: 10.1161/01.res.86.1.59 - PubMed
37. Kobirumaki-Shimozawa F, Oyama K, Shimozawa T, Mizuno A, Ohki T, Terui T, Minamisawa S, Ishiwata S, Fukuda N. Nano-imaging of the beating mouse heart in vivo: importance of sarcomere dynamics, as opposed to sarcomere length per se, in the regulation of cardiac function. J Gen Physiol. 2016;147:53–62. doi: 10.1085/jgp.201511484 - PMC - PubMed
38. Aguirre AD, Vinegoni C, Sebas M, Weissleder R. Intravital imaging of cardiac function at the single-cell level. Proc Natl Acad Sci USA. 2014;111:11257–11262. doi: 10.1073/pnas.1401316111 - PMC - PubMed
39. Bub G, Camelliti P, Bollensdorff C, Stuckey DJ, Picton G, Burton RA, Clarke K, Kohl P. Measurement and analysis of sarcomere length in rat cardiomyocytes in situ and in vitro. Am J Physiol Heart Circ Physiol. 2010;298:H1616–H1625. doi: 10.1152/ajpheart.00481.2009 - PMC - PubMed
40. Gannier F, Bernengo JC, Jacquemond V, Garnier D. Measurements of sarcomere dynamics simultaneously with auxotonic force in isolated cardiac cells. IEEE Trans Biomed Eng. 1993;40:1226–1232. doi: 10.1109/10.250578 - PubMed
41. Yaniv Y, Juhaszova M, Wang S, Fishbein KW, Zorov DB, Sollott SJ. Analysis of mitochondrial 3D-deformation in cardiomyocytes during active contraction reveals passive structural anisotropy of orthogonal short axes. PLoS One. 2011;6:e21985. doi: 10.1371/journal.pone.0021985 - PMC - PubMed
42. Shintani SA, Oyama K, Kobirumaki-Shimozawa F, Ohki T, Ishiwata S, Fukuda N. Sarcomere length nanometry in rat neonatal cardiomyocytes expressed with alpha-actinin-AcGFP in Z discs. J Gen Physiol. 2014;143:513–524. doi: 10.1085/jgp.201311118 - PMC - PubMed
43. Tsukamoto S, Fujii T, Oyama K, Shintani SA, Shimozawa T, Kobirumaki-Shimozawa F, Ishiwata S, Fukuda N. Simultaneous imaging of local calcium and single sarcomere length in rat neonatal cardiomyocytes using yellow Cameleon-Nano140. J Gen Physiol. 2016;148:341–355. doi: 10.1085/jgp.201611604 - PMC - PubMed
44. Louch WE, Koivumaki JT, Tavi P. Calcium signalling in developing cardiomyocytes: implications for model systems and disease. J Physiol. 2015;593:1047–1063. doi: 10.1113/jphysiol.2014.274712 - PMC - PubMed
45. Lichter J, Li H, Sachse FB. Measurement of strain in cardiac myocytes at micrometer scale based on rapid scanning confocal microscopy and non-rigid image registration. Ann Biomed Eng. 2016;44:3020–3031. doi: 10.1007/s10439-016-1593-7 - PMC - PubMed

46. Garcia-Canadilla P, Rodriguez JF, Palazzi MJ, Gonzalez-Tendero A, Schonleitner P, Balicevic V, Loncaric S, Luiken J, Ceresa M, Camara O, et al. . A two dimensional electromechanical model of a cardiomyocyte to assess intra-cellular regional mechanical heterogeneities. PLoS One. 2017;12:e0182915. doi: 10.1371/journal.pone.0182915 - PMC - PubMed
47. Peterson P, Kalda M, Vendelin M. Real-time determination of sarcomere length of a single cardiomyocyte during contraction. Am J Physiol Cell Physiol. 2013;304:C519–C531. doi: 10.1152/ajpcell.00032.2012 - PMC - PubMed
48. Kobirumaki-Shimozawa F, Shimozawa T, Oyama K, Baba S, Li J, Nakanishi T, Terui T, Louch WE, Ishiwata S, Fukuda N. Synchrony of sarcomeric movement regulates left ventricular pump function in the in vivo beating mouse heart. J Gen Physiol. 2021;153:e202012860. doi: 10.1085/jgp.202012860 - PMC - PubMed
49. Hohendanner F, Ljubojevic S, MacQuaide N, Sacherer M, Sedej S, Biesmans L, Wakula P, Platzer D, Sokolow S, Herchuelz A, et al. . Intracellular dyssynchrony of diastolic cytosolic [Ca2+] decay in ventricular cardiomyocytes in cardiac remodeling and human heart failure. Circ Res. 2013;113:527–538. doi: 10.1161/CIRCRESAHA.113.300895 - PubMed
50. Kamgoue A, Ohayon J, Usson Y, Riou L, Tracqui P. Quantification of cardiomyocyte contraction based on image correlation analysis. Cytometry A. 2009;75:298–308. doi: 10.1002/cyto.a.20700 - PubMed
51. Awasthi S, Izu LT, Mao Z, Jian Z, Landas T, Lerner A, Shimkunas R, Woldeyesus R, Bossuyt J, Wood BM, et al. . Multimodal SHG-2PF imaging of microdomain Ca2+-contraction coupling in live cardiac myocytes. Circ Res. 2016;118:e19–e28. doi: 10.1161/CIRCRESAHA.115.307919 - PMC - PubMed
52. Espe EKS, Aronsen JM, Eriksen M, Sejersted OM, Zhang L, Sjaastad I. Regional dysfunction after myocardial infarction in rats. Circ Cardiovasc Imaging. 2017;10:e005997. doi: 10.1161/CIRCIMAGING.116.005997 - PubMed
53. Sachse FB, Torres NS, Savio-Galimberti E, Aiba T, Kass DA, Tomaselli GF, Bridge JH. Subcellular structures and function of myocytes impaired during heart failure are restored by cardiac resynchronization therapy. Circ Res. 2012;110:588–597. doi: 10.1161/CIRCRESAHA.111.257428 - PMC - PubMed
54. de Souza Leite F, Rassier DE. Sarcomere length nonuniformity and force regulation in myofibrils and sarcomeres. Biophys J. 2020;119:2372–2377. doi: 10.1016/j.bpj.2020.11.005 - PMC - PubMed
55. Telley IA, Denoth J, Stussi E, Pfitzer G, Stehle R. Half-sarcomere dynamics in myofibrils during activation and relaxation studied by tracking fluorescent markers. Biophys J. 2006;90:514–530. doi: 10.1529/biophysj.105.070334 - PMC - PubMed
56. Morgan DL. New insights into the behavior of muscle during active lengthening. Biophys J. 1990;57:209–221. doi: 10.1016/S0006-3495(90)82524-8 - PMC - PubMed
57. Lipsett DB, Frisk M, Aronsen JM, Norden ES, Buonarati OR, Cataliotti A, Hell JW, Sjaastad I, Christensen G, Louch WE. Cardiomyocyte substructure reverts to an immature phenotype during heart failure. J Physiol. 2019;597:1833–1853. doi: 10.1113/JP277273 - PMC - PubMed
58. Campbell KS. Interactions between connected half-sarcomeres produce emergent mechanical behavior in a mathematical model of muscle. PLoS Comput Biol. 2009;5:e1000560. doi: 10.1371/journal.pcbi.1000560 - PMC - PubMed
59. Bates D, Machler M, Bolker BM, Walker SC. Fitting linear mixed-effects models using lme4. J Stat Softw. 2015;67:1–48. doi: 10.18637/jss.v067.i01
60. Satterthwaite FE. An approximate distribution of estimates of variance components. Biometrics Bull. 1946;2:110–114. doi: 10.2307/3002019 - PubMed